# Synthesis and Properties of Wholly Aromatic Polymers Bearing Cardo Fluorene Moieties

**GUEY-SHENG LIOU, HUNG-JU YEN, YI-TING SU, HUNG-YI LIN**

Functional Polymeric Materials Research Laboratory, Department of Applied Chemistry, National Chi Nan University, Puli, Nantou Hsien 54561, Taiwan, Republic of China

*Received 4 April 2007; accepted 24 April 2007*
*DOI: 10.1002/pola.22182*
*Published online in Wiley InterScience (www.interscience.wiley.com).*

**ABSTRACT:** Three series of aromatic polyamides, polyesters, and poly(1,3,4-oxadiazole)s containing bulky fluorene structures were prepared from 9,9-bis(4-carboxyphenyl) fluorene. All of the polymers were readily soluble in many organic solvents and showed useful thermal stability associated with high glass-transition temperatures in the range of 220–366 °C. These wholly aromatic polymer films were colorless, with high optical transparency, and exhibited UV-vis absorption bands at 266–348 nm and photoluminescence maximum bands at 368–457 nm within the purple to green region in *N,N*-dimethylacetamide (DMAc) solutions. The poly(amine-amide) **Ic** exhibited excellent electrochromic contrast and coloration efficiency, changing color from the colorless neutral form to green and then to the dark blue oxidized forms with good stability of electrochromic characteristics. Almost all of these wholly aromatic polymer films were colorless and showed high optical transparency. © 2007 Wiley Periodicals, Inc. J Polym Sci Part A: Polym Chem 45: 4352–4363, 2007

**Keywords:** electrochemistry; functionalization of polymers; high performance polymers; polyamides; polycondensation

## INTRODUCTION

In the past decade, fluorene-based $\pi$-conjugated polymers (PFs) have emerged as a very promising class of blue-light emitting materials for use in polymer light-emitting diodes (PLEDs) because of their highly efficient photoluminescence (PL) and electroluminescence (EL), thermal stability, good solubility, and facile functionalization at C-9 position of fluorine.[1–4] The high fluorenscence yields and blue emission of polymers involving 2,7-linked fluorene units make them among the most attractive classes of conjugated polymers for devices[2,5] and good candidates for the above applications. It is thus worthwhile to design a fluorene-based aromatic dicarboxylic acid as a starting monomer for the preparation of high-performance polymers.

Wholly aromatic polyamides (aramids), polyesters (polyarylates), and poly(1,3,4-oxadiazole)s are characterized as highly thermally stable polymers with a favorable balance of physical and chemical properties. However, the rigidity of the backbone and strong hydrogen-bonding in polyamides result in high melting temperatures or glass-transition temperatures and limited solubility in most organic solvents thus restricting their applications in some fields.[6–10] To overcome these limitations, polymer-structure modification becomes necessary. One of the common approaches for increasing the solubility and processability of these polymers without sacrificing high thermal stability is the introduction of bulky, packing-disruptive groups into the polymer backbone.[11–17]

*Correspondence to:* G.-S. Liou (E-mail: gsliou@ncnu.edu.tw)

Journal of Polymer Science: Part A: Polymer Chemistry, Vol. 45, 4352–4363 (2007)

Polyarylates possess high optical transparency and excellent mechanical properties. So far, however, most studies have focused on their high-performance applications. There is no application using polyarylates as photonic/electronic device materials. Thus, modulation of their photophysical and electrical properties by means of a simple condensation synthetic method may be an impressive challenge in terms of new development of PLEDs materials.

1,3,4-Oxadiazole-containing conjugated polymers have been widely investigated and applied as electron transport or emission layers in PLEDs.[18–22] Unfortunately, aromatic polyoxadiazoles are difficult to process owing to their infusible and insoluble properties and their tendency to be brittle. To overcome these limitations, we recently reported the synthesis of soluble aromatic polyoxadiazoles by incorporation of bulky phenyl or naphthyl and propeller-shaped triarylamine units into the polymer backbone.[23,24] The obtained polymers were amorphous with good solubility in many organic solvents, excellent film-forming capability, and high thermal stability.

In this article, we synthesized three series of fluorene-containing aromatic polyamides, polyesters, and poly(1,3,4-oxadiazole)s based on 9,9-bis(4-carboxyphenyl)fluorene. These polymers are expected to exhibit high optical transparency with good solubility because of the introduction of cardo fluorene structure along polymer main chain. The general properties such as solubility and thermal properties are reported. The photoluminescent, electrochemical, and electrochromic properties of some of these polymers are also described herein.

## EXPERIMENTAL

### Materials

*N,N*-Bis(4-aminophenyl)-*N′,N′*-diphenyl-1,4-phenylenediamine (**3c**) (m.p.: 245–247 °C) was synthesized according to the reported procedure.[25] 4,4′-Oxydianiline (**3a**) (TCI), 9,9-bis(4-aminophenyl)fluorene (**3b**) (TCI), 4,4′-dihydroxydiphenyl ether (**4a**) (TCI), 9,9-bis(4-hydroxyphenyl)fluorene (**4b**) (TCI), 4,4′-isopropylidenediphenol (bisphenol A) (**4c**) (Acros), terephthalic dihydrazide (**5-TPH**) (TCI), and isophthalic dihydrazide (**5-IPH**) (TCI) were used without further purification. Commercially obtained anhydrous calcium chloride ($CaCl_2$) was dried under vacuum at 180 °C for 8 h. Tetrabutylammonium perchlorate (TBAP) (Acros) were recrystallized twice from ethyl acetate and then dried *in vacuo* prior to use. All other reagents were also used as received from commercial sources.

### Monomer Synthesis

#### *9,9-Bis(4-cyanophenyl)fluorene (1)*

A mixture of 10.0 g (60.2 mmol) of fluorene, 15 mL of toluene, 50 mL of DMF, 8.20 g (31.0 mmol) of 18-crown-6-ether, 19.80 g (144.4 mmol) of potassium carbonate, and 16.25 g (134.1 mmol) of 4-fluorobenzonitrile were added in sequence under nitrogen atmosphere. The mixture was heated with stirring at 140 °C for 3.5 h to remove water and toluene, and then the reaction continued for 6 h. After cooling, the solution was dropped into 600-mL of ice water. The product was filtered and recrystallized from tetrahydrofuran (THF) to afford 14.23 g (64% in yield) of light yellow lump crystals with a melting point (mp) of 284–286 °C (by DSC at 10 °C/min). IR (KBr): 2229 $cm^{-1}$ (C≡N stretch).

$^1$H NMR (DMSO-$d_6$, $\delta$, ppm): 7.27 (d, 4H), 7.33 (t, 2H), 7.42–7.47 (m, 4H), 7.74 (d, 4H), 7.53 (d, 2H). $^{13}$C NMR (DMSO-$d_6$, $\delta$, ppm): 65.3, 110.2, 118.8 (—C≡N), 121.2, 126.2, 128.6, 128.8, 132.8, 139.9, 148.6, 150.4.

#### *9,9-Bis(4-carboxyphenyl)fluorene (2)*

A mixture of 10.91 g (194.4 mmol) of potassium hydroxide and 5.12 g (13.9 mmol) of the obtained dinitrile compound **1** in 35 mL of ethanol and 35 mL of distillated water was stirred at ~100 °C until no further ammonia was generated. The time taken to reach this stage was about 4 days. The solution was cooled and the pH value was adjusted by dilute hydrochloric acid to near 3. The white precipitate formed was collected by filtration, washed thoroughly with water, and recrystallized by acetic acid to give 4.56 g (80% in yield) of white crystals with a mp of 359–360 °C (by DSC at 10 °C/min) (lit:[26] 164–165 °C). IR (KBr): 1690 (C=O stretch), 2700–3200 $cm^{-1}$ (O—H stretch). $^1$H NMR (DMSO-$d_6$, $\delta$, ppm): 7.22 (d, 4H), 7.33 (t, 2H), 7.40–7.48 (m, 4H), 7.84 (d, 4H), 7.96 (d, 2H), 12.80 (s, 2H, OH). $^{13}$C NMR (DMSO-$d_6$, $\delta$, ppm): 65.3, 121.0, 126.3, 128.0, 128.4, 129.7, 129.8, 139.9, 149.6, 150.3, 167.2 (C=O).

## Polymer Synthesis

### *Synthesis of Polyamides*

The synthesis of polyamide **Ia** is used as an example to illustrate the general synthetic route. A mixture of 0.406 g (1.0 mmol) of 9,9-bis(4-carboxyphenyl)fluorene (**2**), 0.200 g (1.0 mmol) of 4,4′-diaminodiphenyl ether (**3a**), 0.12 g of calcium chloride, 0.7 mL of triphenyl phosphite (TPP), 0.5 mL of pyridine, and 1.0 mL of *N*-methyl-2-pyrrolidone (NMP) was heated with stirring at 105 °C for 3 h. The polymer solution obtained was poured slowly into 200 mL of stirring methanol giving rise to a stringy fiber-like precipitate that was collected by filtration, washed thoroughly with hot water and methanol, and dried under vacuum at 100 °C. Reprecipitation from DMAc poured into methanol was carried out twice for further purification to give 0.56 g (99% in yield). The inherent viscosity of the obtained polyamides **Ia** was 0.55 dL/g, measured at a concentration of 0.5 g/dL in DMAc at 30 °C. The IR spectrum of **Ia** (film) exhibited characteristic amide absorption bands at 3285 $cm^{-1}$ (N—H stretching), 1650 $cm^{-1}$ (amide carbonyl).

$^1$H NMR (DMSO-$d_6$, $\delta$, ppm): 6.99 (d, 4H, $H_h$), 7.28 (d, 4H, $H_e$), 7.35 (t, 2H, $H_b$), 7.43 (t, 2H, $H_c$), 7.51 (d, 2H, $H_a$), 7.75 (d, 4H, $H_g$), 7.85 (d, 4H, $H_f$), 7.97 (d, 2H, $H_d$), 10.25 (s, 2H, amide-NH). $^{13}$C NMR (DMSO-$d_6$, $\delta$, ppm): 64.5 ($C^1$), 118.1 ($C^{14}$), 120.4 ($C^6$), 121.5 ($C^{13}$), 125.6 ($C^3$), 127.2 ($C^{10}$), 127.4 ($C^9$), 127.7 ($C^4$ + $C^5$), 133.4 ($C^{12}$), 134.2 ($C^{11}$), 139.2 ($C^7$), 148.2 ($C^8$), 149.2 ($C^2$), 152.4 ($C^{15}$), 164.7 (amide carbonyl).

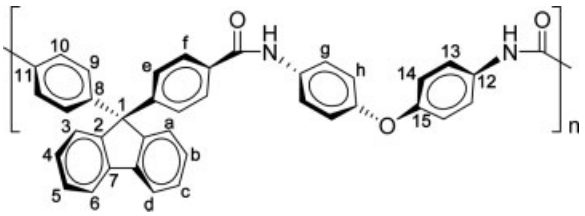


### *Synthesis of Polyarylates*

A solution of diphenylchlorophosphate (DPCP) (0.69 g), LiCl (0.09 g), and pyridine (3.0 mL) was stirred at room temperature for 30 min and then added drop wise for 20 min to a hot solution (preheated at 120 °C for 5 min) containing 0.406 g (1.0 mmol) of 9,9-bis(4-carboxyphenyl)-fluorene (**2**) and 0.202 g (1.0 mmol) of 4,4′-dihydroxydiphenyl ether (**4a**) in pyridine (2.0 mL). The final solution was heated at 120 °C for 3 h and the obtained polymer solution was poured slowly into 200 mL of stirring methanol, giving a powder-like precipitate that was collected by filtration, washed thoroughly with hot water and methanol, and dried under vacuum at 100 °C. Reprecipitation from DMAc poured into methanol was carried out twice for further purification to give 0.56 g (98% in yield). The inherent viscosity of the obtained polyarylate **IIa** was 0.21 dL/g measured at a concentration of 0.5 g/dL in DMAc at 30 °C.

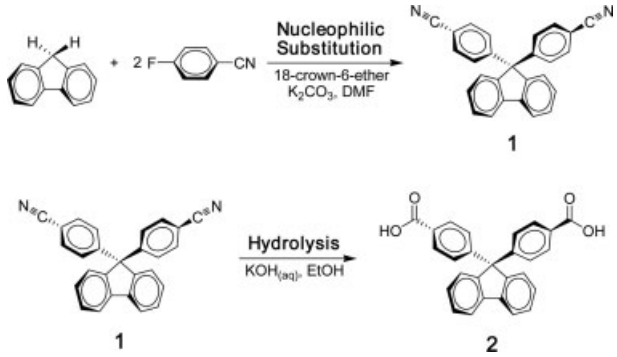


**Scheme 1.** Synthesis of cardo fluorene-based monomers.

The IR spectrum of **IIa** (film) exhibited characteristic ester absorption bands at 1734 $cm^{-1}$ (C=O stretch) and 1200–1270 $cm^{-1}$ (C—O stretch). $^1$H NMR (DMSO-$d_6$, $\delta$, ppm): 7.08 (d, 4H), 7.24 (d, 4H), 7.33 (d, 6H), 7.43–7.50 (m, 4H), 7.96–8.03 (m, 6H). $^{13}$C NMR (DMSO-$d_6$, $\delta$, ppm): 65.5, 119.7, 121.1, 123.7, 126.3, 127.9, 128.4, 130.4, 140.0, 146.4, 149.3, 151.5, 154.6, 164.6 (ester carbonyl).

### *Synthesis of Polyhydrazides*

The polyhydrazides were synthesized from dicarboxylic acid monomer **2** and dihydrazides, **5-TPH** and **5-IPH**, via phosphorylation polycondensation method. A typical synthetic procedure for polyhydrazide **III-IPH** is described as follows. A dried 50-mL flask was charged with **2** 0.406 g (1.0 mmol), **5-IPH** 0.194 g (1.0 mmol), NMP (2.00 mL), calcium chloride(0.24 g), diphenyl phosphite (DPP) (0.80 mL), and pyridine (0.48 mL). The mixture was heated with stirring at 120 °C for 5 h. As polycondensation proceeded, the solution became viscous gradually. The resulting viscous polymer solution was

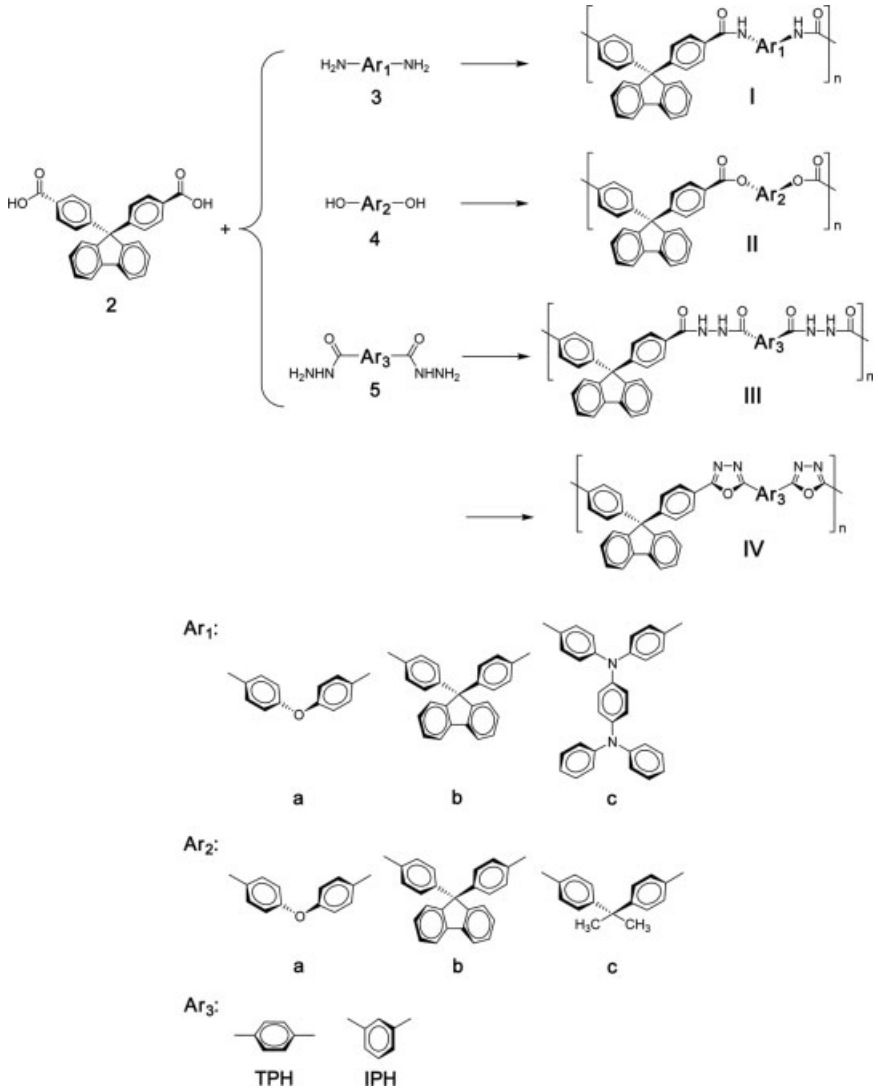


**Scheme 2.** Synthesis of cardo fluorene-based polymers.

poured slowly into 300 mL of methanol, giving a powder-like precipitate that was collected by filtration, washed thoroughly with hot water and methanol. Reprecipitation by DMAc/methanol was carried out twice for further purification to give 0.55 g (97% in yield). The yield was quantitative and the inherent viscosity of polyhydrazide **III-IPH** was 0.21 dL/g measured in DMAc at a concentration of 0.5 g/dL at 30 °C. IR (film): 3265 $cm^{-1}$ (*N*-H), 1648 $cm^{-1}$ (C=O).

$^{1}H$ NMR (DMSO-$d_6$, $\delta$, ppm): 7.28 (d, 4H), 7.36 (t, 2H), 7.45 (t, 2H), 7.29 (d, 2H), 7.66 (t, 1H), 7.85 (d, 4H), 7.99 (d, 2H), 8.09 (d, 2H), 8.46 (s, 1H), 10.57 (hydrazide-NH). $^{13}C$ NMR (DMSO-$d_6$, $\delta$, ppm): 65.2, 121.1, 126.3, 127.3, 128.0, 128.4, 129.1, 130.8, 131.4, 133.2, 139.9, 149.3, 149.7, 165.5 (hydrazide carbonyl).

### *Film Preparation and Cyclodehydration of the Polyhydrazides*

A solution of polymer was made by dissolving about 0.5 g of the polymer sample in 6 mL of DMAc. The homogeneous solution was poured into a 9-cm glass Petri dish, which was heated at 60 °C for 2 h, 130 °C for 2 h, and 160 °C for 4 h to slowly release the solvent under vacuum. The obtained films were about 6–15 $\mu$m in thickness and were used for solubility tests, optical properties, and thermal analyses.

The cyclodehydration of the polyhydrazide **III-IPH** to the corresponding polyhydrazide **IV-IPH** was carried out by successive heating the above fabricated polymer films at 200 °C for 30 min, 300 °C for 1 h, and then 350 °C for 3 h under vacuum.

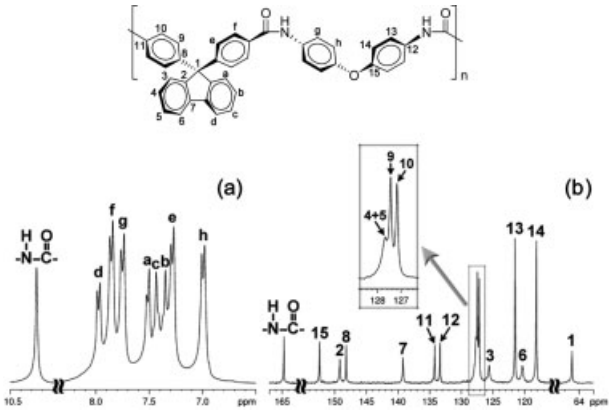

**Figure 1.** (a) $^{1}$H NMR and (b) $^{13}$C NMR spectrum of polyamide **Ia** in DMSO-$d_6$.

## Measurements

Infrared spectra were recorded on a Perkin–Elmer RXI FT-IR spectrometer. $^{1}$H and $^{13}$C NMR spectra were measured on a Bruker Avance 300 MHz FT NMR system and referenced to the DMSO-$d_6$ signal, and peak multiplicity was reported as follows: s, singlet; d, doublet; t, triplet; m, multiplet. The inherent viscosities were determined at 0.5 g/dL concentration using a Tamson TV-2000 viscometer at 30 °C. Thermogravimetric analysis (TGA) was conducted with a Perkin–Elmer Pyris 1 TGA. Experiments were carried out on ~6–8 mg film samples heated in flowing nitrogen or air (flow rate: 30 cm$^3$/min) at a heating rate of 20 °C/min. DSC analyses were performed on a Perkin–Elmer Pyris 1 DSC, and $T_g$ was the midpoint temperature of baseline shift on the second DSC heating trace (rate: 20 °C/min) of the sample after quenching from 400 to 50 °C (rate: 200 °C/min) in flowing nitrogen (30 cm$^3$/min). Ultraviolet-visible (UV-Vis) spectra of the polymer films were recorded on a Varian Cary 50 Probe spectrometer. Absorption spectra were measured with a HP 8453 UV-Visible spectrophotometer. Photoluminescence spectra were measured with a Jasco FP-6300 spectrofluorometer (thickness: 3–6 $\mu$m). Photoluminescence quantum yield ($\Phi_{PL}$) of the samples in DMAc were measured by using quinine sulfate (dissolved in 1 N sulfuric acid with a concentration of $10^{-5}$ M, assuming photoluminescence quantum efficiency of 0.546) as a standard at 24–25 °C.[27] All corrected fluorescence excitation spectra were found to be equivalent to their respective absorption spectra. Electrochemistry was performed with a CHI 611B electrochemical analyzer. Voltammograms are presented with the positive potential pointing to the left and with increasing anodic currents pointing downwards. Cyclic voltammetry was performed with the use of a three-electrode cell in which ITO (polymer films area about 0.7 cm × 0.5 cm) was used as a working electrode and a platinum wire as an auxiliary electrode at a scan rate of 100 mV/s against a Ag/AgCl reference electrode in acetonitrile ($CH_3CN$) solution of 0.1 M tetrabutylammonium perchlorate (TBAP) under nitrogen atmosphere for oxidation measurement. Voltammograms are presented with the positive potential pointing to the right and with increasing anodic currents pointing upwards. The spectroelectrochemical

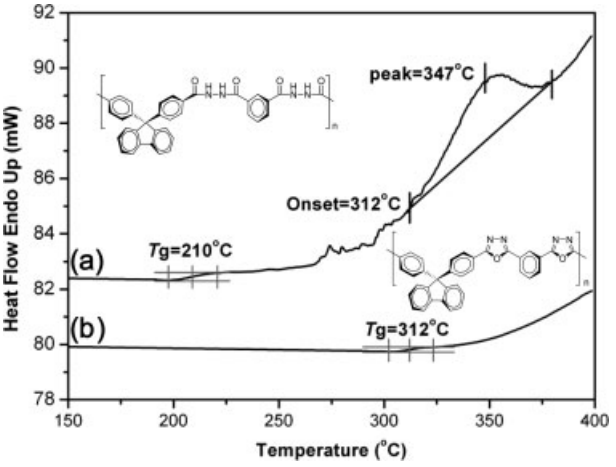


**Figure 2.** DSC traces of (a) polyhydrazide **III-IPH** and (b) poly(1,3,4-oxadiazole) **IV-IPH** with a heating rate of 20 °C/min in nitrogen.

**Table 1.** Thermal Properties of Aromatic Polymers[a]

| Polymer | $T_g$ (°C) | $T_d$ at 5 % Weight Loss (°C) | | $T_d$ at 10 % Weight Loss (°C) | | Char Yield (wt %)[b] |
|---|---|---|---|---|---|---|
| | | $N_2$ | Air | $N_2$ | Air | |
| **Ia** | 318 | 540 | 530 | 620 | 595 | 78 |
| **Ib** | 366 | 525 | 525 | 595 | 590 | 70 |
| **Ic** | 322 | 540 | 520 | 620 | 590 | 75 |
| **IIa** | 220 | 495 | 470 | 550 | 530 | 55 |
| **IIb** | 265 | 510 | 490 | 550 | 540 | 61 |
| **IIc** | 242 | 485 | 470 | 540 | 520 | 50 |

[a] The polymer film samples were heated at 200 °C for 1 h prior to all the thermal analyses.
[b] Residual weight percentage at 800 °C in nitrogen.

**Table 2.** Thermal Properties of Aromatic Polymers[a]

| Poly(amine-hydrazide)s[b] | | | | Poly(amine-1,3,4-oxadiazole)s | | | | | | |
|---|---|---|---|---|---|---|---|---|---|---|
| | | | | | | $T_d$ at 5 % Weight Loss (°C) | | $T_d$ at 10 % Weight Loss (°C) | | |
| Code | $T_g$ (°C) | $T_o$ (°C) | $T_p$ (°C) | Code | $T_g$ (°C) | $N_2$ | Air | $N_2$ | Air | Char Yield (wt %)[c] |
| **III-TPH** | 258 | 328 | 390 | **IV-TPH** | 320 | 540 | 535 | 565 | 560 | 68 |
| **III-IPH** | 210 | 312 | 380 | **IV-IPH** | 312 | 520 | 515 | 540 | 535 | 61 |

[a] The polymer film samples were heated at 200 °C for 1 h prior to all the thermal analyses.
[b] DSC data obtained from the DSC heating traces with a heating rate of 20 °C/min in nitrogen. $T_g$, the midpoint of baseline shift on the first DSC trace; $T_o$, extrapolated onset temperature of the endothermic peak; $T_p$, endothermic peak temperature.
[c] Residual weight percentage at 800 °C in nitrogen.

cell was composed of a 1 cm cuvette, ITO as a working electrode, a platinum wire as an auxiliary electrode, and a home-made Ag/AgCl, KCl (sat.) reference electrode.

## RESULTS AND DISCUSSION

### Monomer Synthesis

9,9-Bis(4-cyanophenyl)fluorene (**1**) was synthesized from the fluorene and 4-fluorobenzonitrile by nucleophilic substitution reaction (Scheme 1), and 9,9-bis(4-carboxyphenyl)fluorene (**2**) could be readily prepared by hydrolysis of compound (**1**) in alkaline solution according to the reported procedure.[26] IR, $^1$H and $^{13}$C NMR spectroscopic techniques were used to identify structures of the intermediate compounds **1** and **2** and agree well with the proposed molecular structures.

### Polymer Synthesis

Three series of aromatic polyamides, polyesters, and new poly(1,3,4-oxadiazole)s with cardo fluorene structures were prepared from 9,9-bis(4-carboxyphenyl)fluorene as showed in Scheme 2. The polymerization was homogeneous throughout the reaction and afforded viscous polymer solutions. The formation of these polymers was confirmed by IR and NMR spectroscopy. As a representative example, a typical set of $^1$H and $^{13}$C NMR spectra of **Ia** in DMSO-$d_6$ are showed in Figure 1, where all the peaks have been readily assigned to the hydrogen and carbon atoms of the recurring unit.

Thermal conversion of the hydrazide group to the 1,3,4-oxadiazole ring was confirmed with IR spectroscopy. As a representative study, a thin-film sample of polyhydrazide **III-IPH** was heated at 350 °C for 3 h. The IR spectra was shown that the cyclization of polyhydrazide **III-IPH** to poly(1,3,4-oxadiazole) **IV-IPH** was confirmed by the disappearance of the absorption at 3246 (hydrazide *N*-H), 1657 cm$^{-1}$ (hydrazide carbonyl), and exhibited the characteristic 1,3,4-oxadiazole ring vibration at around 1488, 1602 (C=N), and 1072 cm$^{-1}$ (C—O—C). DSC also could be used to investigate the cyclization process. A typical pair of DSC curves of polyhydrazide **I-IPH** and poly(1,3,4-oxadiazole) **III-IPH** are illustrated in Figure 2. The main endothermic peak revealed the cyclodehydration reaction of hydrazide group with water evolution in the range of 300–400 °C.

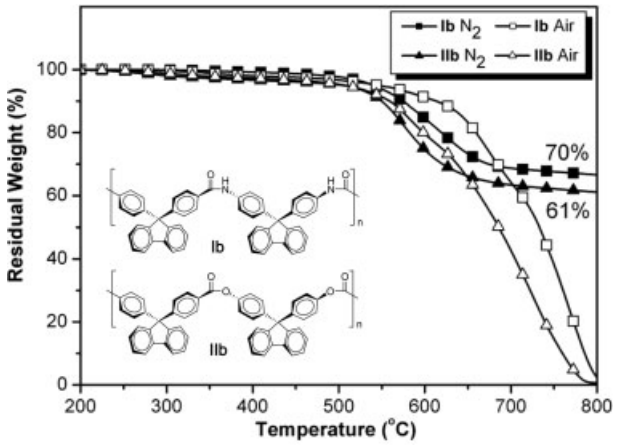


**Figure 3.** TGA thermograms of polymer **Ib** and **IIb** at a scan rate of 20 °C/min.

**Table 3.** Inherent Viscosity[a] and Optical Properties for Aromatic Polymers

| | | DMAc ($1 \times 10^{-5}$ M) Solution, R.T. | | | Film (nm), R.T. | | | | |
|---|---|---|---|---|---|---|---|---|---|
| Index | $\eta_{inh}$ (dL/g) | $\lambda_{abs}$ (nm) | $\lambda_{em}$ (nm)[b] | $\Phi_{PL}$ (%) | $\lambda_0$[c] | $\lambda_{abs}$ | $\lambda_{onset}$ | $\lambda_{em}$[b] | $E_g$[d] (eV) |
| **Ia** | 0.55 | 286 | 452 | 3.8 | 299 | 295 | 346 | 452, 479 | 3.58 |
| **Ib** | 0.44 | 278, 308[e] | 454 | 2.1 | 346 | 295 | 333 | 451, 479 | 3.72 |
| **Ic** | 0.36 | 275, 309, 348[e] | 456 | 3.6 | 391 | 297, 310, 345[e] | 409 | 512, 520 | 3.03 |
| **IIa** | 0.21 | 267, 308[e] | 443 | 6.1 | 311 | 291, 310[e] | 319 | 451, 481 | 3.89 |
| **IIb** | 0.17 | 267, 309[e] | 455 | 7.8 | 296 | 291, 310[e] | 320 | 449, 480 | 3.88 |
| **IIc** | 0.17 | 267, 308[e] | 456 | 8.2 | 309 | 291, 310[e] | 318 | 449, 478 | 3.90 |
| **III-TPH** | 0.30 | 267, 309[e] | 448 | 2.8 | 326 | 290, 310[e] | 325 | 453, 483 | 3.82 |
| **III-IPH** | 0.21 | 267, 309[e] | 457 | 4.5 | 311 | 291, 310[e] | 321 | 451, 483 | 3.86 |
| **IV-TPH** | 0.26 | 267, 309[e] | 382 | 9.7 | 357 | 299, 310[e] | 376 | 479 | 3.30 |
| **IV-IPH** | 0.21 | 266, 309[e] | 368 | 14.2 | 333 | 295, 310[e] | 350 | 497 | 3.54 |

[a] Measured at a polymer concentration of 0.5 g/dL in DMAc at 30 °C. (**IV** series were measured in concentrated sulfuric acid).
[b] They were excited at $\lambda_{abs}$ for both solid and solution states.
[c] The cutoff wavelength from the UV-Vis transmission spectra of polymer films.
[d] The data were calculated from polymer film by the equation: gap = $1240/\lambda_{onset}$.
[e] Excitation wavelength for PL and $\Phi_F$ measurement.

## Polymer Properties

### *Basic Characterizations*

These polymers **I–III** exhibited excellent solubility in common organic solvents such as NMP, DMAc, DMSO, and DMF. The polyarylate **II** series were even soluble in THF and $CHCl_3$. The lost of solubility derived from the dehydration of **III** to give an even more rigid structure. The enhanced solubility can be attributed to the introduction of bulky cardo fluorene group in the repeat unit which decreases interchain interaction and increases the free volume between polymer main chains. Thus, the excellent solubility makes these polymers as potential candidates for practical applications by spin- or dip-coating processes.

The thermal properties of the polyamides were investigated by TGA and DSC. The results are summarized in Tables 1 and 2. Typical TGA curves of representative polymers **Ib** and **IIb** in both nitrogen and air atmospheres are shown in Figure 3. All the aromatic polymers exhibited good thermal stability with insignificant weight loss up to 500 °C in nitrogen. The 10% weight-loss temperatures of the aromatic polymers in nitrogen and air were recorded in the range of 540–620 °C and 520–595 °C, respectively. The

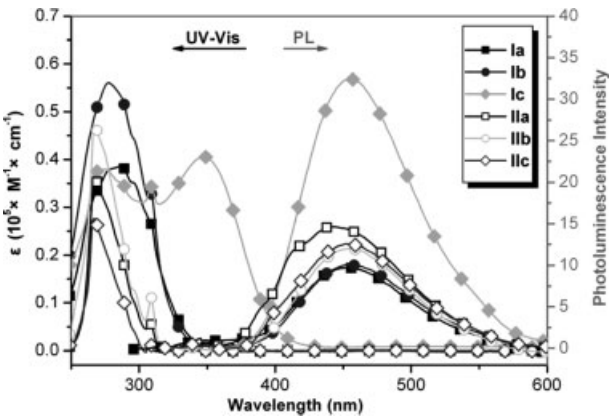


**Figure 4.** Molar absorptivity (left) and photoluminescence intensity (right) of polymers **I** and **II** in DMAc solution (*ca.* $1 \times 10^{-5}$ M).

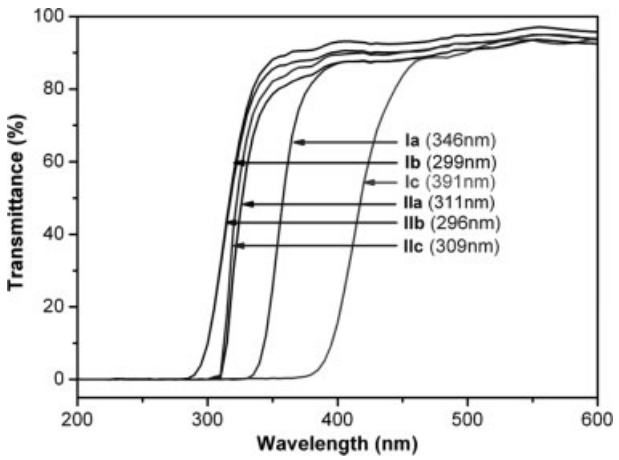


**Figure 5.** UV-Visible transmission spectrum of polymer **I** and **II** films.

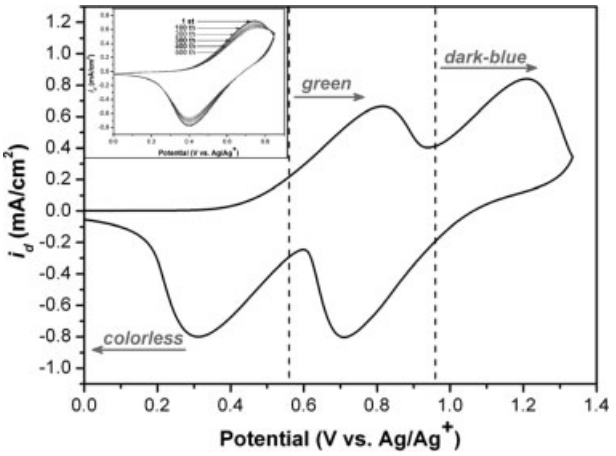


**Figure 6.** Cyclic voltammograms of polyamide **Ic** film with 500 cyclic scans on an ITO-coated glass substrate in $CH_3CN$ solutions containing 0.1 M TBAP at a scan rate of 100 mV/s. The arrows indicate the film color change during scan. $E_{1/2}$ values are indicated by dashed lines.

amount of carbonized residue (char yield) of these polymer in nitrogen atmosphere was more than 50% at 800 °C. The high char yields of these polymers can be ascribed to their high aromatic content. The $T_g$ of all the aromatic polymers could be easily measured in the DSC thermograms that were observed in the range of 220–366 °C, and indicated no clear melting endotherms up to the decomposition temperatures.

### *Optical and Electrochemical Properties*

Table 3 lists the solubility behavior and optical properties of polymer **I–IV** series, which were investigated by UV-Vis and photoluminescence spectroscopy. Figure 4 shows molar absorptivity ($\varepsilon$) and photoluminescence (PL) spectra of the aromatic polymers **I** and **II** measured in DMAc solution (Conc.: $10^{-5}$ M). These polymers exhibited UV-Vis absorption bands at 266–348 nm in DMAc solution and showed maximum photoluminescence bands at 368–457 nm with quantum yield ranging from 2.1 to 14.2%. In the solid state, the UV-Vis absorption and photoluminescence spectra of polymer **I–IV** series except **Ic** are nearly identical and show maxima absorbance at 295–310 nm, and the cutoff wavelengths (absorption edge; $\lambda_0$) were in the range of 296–357 nm showing almost colorless and high optical transparency (Fig. 5).

The electrochemical oxidation redox behavior of new polyamide **Ic** was investigated by cyclic voltammetry conducted by the cast film on an ITO-coated glass substrate as working electrode in dry acetonitrile ($CH_3CN$) containing 0.1 M of TBAP as an electrolyte under a nitrogen atmosphere. The cyclic voltammograms for polyamide **Ic** are shown in Figure 6. There are two reversible oxidation redox couples at $E_{1/2} = 0.56$ ($E_{onset} = 0.46$ V) and 0.96 V, respectively, and exhibit good electrochemical stability during continuous 500 cyclic scans. The electron removal in the first stage for polyamide **Ic** is assumed to occur at the N atom surrounded by two phenyl groups with electron-donating amide linkages in the main chain, which is more electron-rich than the N atom surrounded only by two phenyl units at the side chain.[25,28] The energy level of the highest occupied molecular orbital (HOMO) and lowest unoccupied molecular orbital (LUMO) of polymer **Ic** could be determined from the oxidation onset potential ($E_{onset}$) and onset absorption wavelength of the polymer film, and the results are also listed in Table 4. The oxidation onset

**Table 4.** Electrochemical Properties for Polyamide **Ic**

| Index | $\lambda_{onset}$[a] | Oxidation/V (vs. Ag/AgCl in $CH_3CN_{(aq)}$) $E_{1/2}^{Ox,1}$[b] | $E_{1/2}^{Ox,2}$[b] | $E_{onset}^{Ox}$ | $E_g$ (eV)[c] | $E_{HOMO}$[d] (eV) | $E_{LUMO}$ (eV) |
|---|---|---|---|---|---|---|---|
| **Ic** | 409 | 0.56 | 0.96 | 0.46 | 3.03 | 4.82 | 1.79 |

[a] The cutoff wavelength from the UV-Vis transmission spectra of polymer films.
[b] Half-wave potentials (average potential of the redox couple peaks).
[c] The data were calculated from polymer films by the equation: $E_g = 1240/\lambda_{onset}$ (energy gap between HOMO and LUMO).
[d] The LUMO energy levels were calculated from cyclic voltammetry and were referenced to ferrocene (4.8 eV).

**Table 5.** Electrochemical Properties for Poly(1,3,4-oxadiazole)s

| Index | $\lambda_{onset}$[a] | Reduction/V (vs. Ag/AgCl in $DMF_{(aq)}$) $E_{1/2}^{Re,1b}$ | $E_{1/2}^{Re,2b}$ | $E_{onset}^{Re}$ | $E_g$ (eV)[c] | $E_{HOMO}$ (eV) | $E_{LUMO}$[d] (eV) |
|---|---|---|---|---|---|---|---|
| **IV-TPH** | 376 | −1.43 | −1.91 | −1.40 | 3.30 | 6.26 | 2.96 |
| **IV-IPH** | 350 | −1.73 | –[e] | −1.67 | 3.54 | 6.23 | 2.69 |

[a] The cutoff wavelength from the UV-Vis transmission spectra of polymer films.
[b] Half-wave potentials (average potential of the redox couple peaks).
[c] The data were calculated from polymer films by the equation: $E_g = 1240/\lambda_{onset}$ (energy gap between HOMO and LUMO).
[d] The LUMO energy levels were calculated from cyclic voltammetry and were referenced to ferrocene (4.8 eV).
[e] The second reduction process could not be measured.

potential for polyamide **Ic** has been determined as 0.46 V versus Ag/AgCl from Figure 6, and the external ferrocene/ferrocenium ($Fc/Fc^+$) redox standard $E_{1/2}$ ($Fc/Fc^+$) is 0.44 V versus Ag/AgCl in $CH_3CN$. Assuming that the HOMO energy level for the $Fc/Fc^+$ standard is 4.80 eV with respect to the zero vacuum level, the HOMO value for polyamide **Ic** could be evaluated to be 4.82 eV.

The electrochemical properties of the poly(1,3,4-oxadiazole)s were also investigated and summarized in Table 5. The reduction behavior of these polymers was investigated by cyclic voltammetry conducted for the cast films on an ITO-coated glass substrate as working electrode in dry and *N,N*-dimethylformamide (DMF) containing 0.1 M of TBAP as an electrolyte under nitrogen atmosphere. Figure 7 shows the typical cyclic voltammograms for poly(1,3,4-oxadiazole)s **IV-TPH**, **IV-IPH**. The poly(1,3,4-oxadiazole)s **IV-TPH** undergo two reduction processes at $E_{1/2} = -1.43$ ($E_{onset} = -1.40$ V) and −1.91 V. The mechanism for the electrochemical reduction of poly(1,3,4-oxadiazole)s could be depicted as in Scheme 3.[29] The LUMO value for poly(1,3,4-oxadiazole) **IV-TPH** was evaluated to be 2.96 eV.

### *Electrochromic Characteristics*

Electrochromism of the polyamide **Ic** thin film was examined by casting polymer solution onto an indium-tin oxide (ITO)-coated glass substrate, and its electrochromic transmittance spectra was monitored by a UV-Vis spectrometer at different applied potentials. The electrode preparations and solution conditions were identical to those used in cyclic voltammetry. The typical electrochromic transmittance spectra of polyamides **Ic** are shown in Figures 8–10. When the applied potentials increased positively from 0.0 to 0.95 V, the peak of characteristic absorbance at 345 nm for polyamide **Ic** decreased gradually while new bands grew up at 425 and 975 nm due to the first stage oxidation, and the color of film changed from original colorless to green. When the potentials were adjusted to more positive values corresponding to second stage oxidation, the characteristic peaks for polyamide$^+$ disappeared gradually and a new band grew up at 730 nm. The new spectrum was assigned as polyamide$^{2+}$ and the color of the film became dark blue. Furthermore, the transmittance mod-

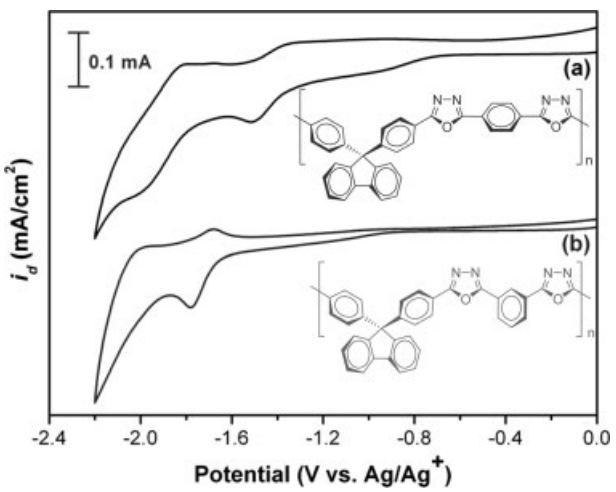


**Figure 7.** Cyclic Voltammograms of poly(1,3,4-oxadiazole)s (a) **IV-TPH**, and (b) **IV-IPH** films onto an indium-tin oxide (ITO)-coated glass substrate in dry DMF solution containing 0.1 M TBAP at scan rate = 0.3 V/s.

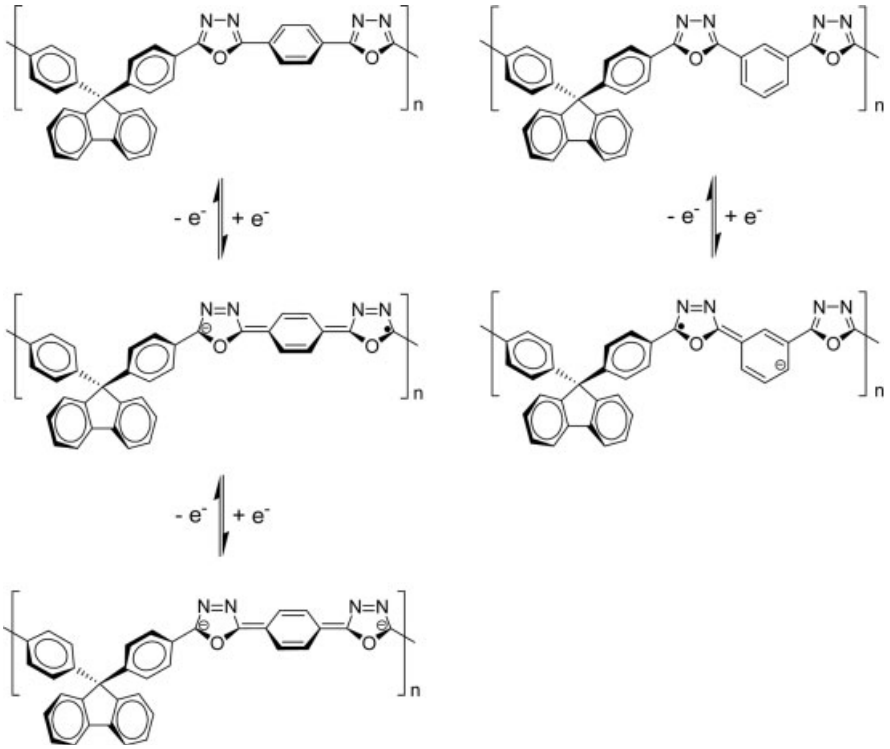

**Scheme 3.** Reaction scheme of the electrochemical reduction of poly(1,3,4-oxadiazole)s in an aprotic medium.

ulation at 975 and 730 nm showing very high contrast values, about 60 and 89%, are also shown in Figures 8–10, respectively. The high coloration efficiency (299 $cm^2/C$) at 975 nm with high optical density change ($\delta OD$) up to 0.46 and low charge ($Q$) (1.53 $mC/cm^2$) could be

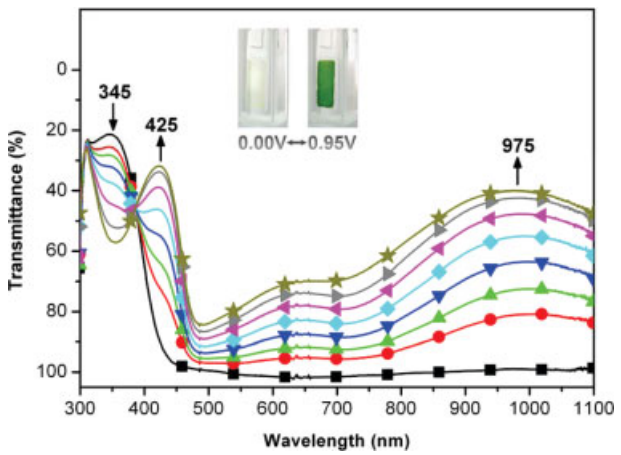


**Figure 8.** Electorchromic behavior of **Ic** thin film (in $CH_3CN$ with 0.1 M TBAP as the supporting electrolyte) at 0.00 (■), 0.60 (●), 0.65 (▲), 0.70 (▼), 0.75 (◆), 0.80 (◀), 0.85 (▶), and 0.95 (★) (V versus $Ag/Ag^+$) for first stage oxidation. [Color figure can be viewed in the online issue, which is available at www.interscience.wiley.com.]

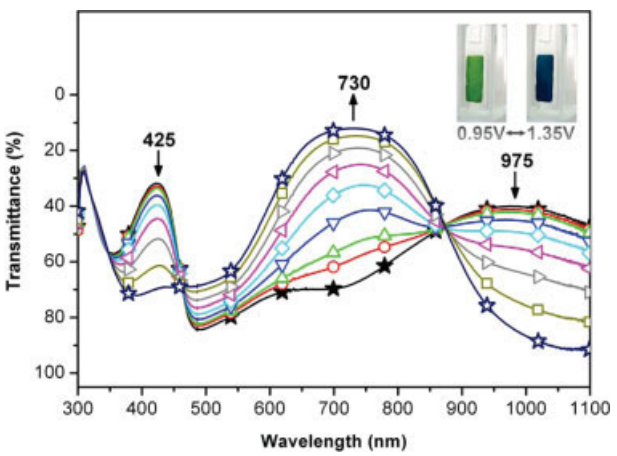


**Figure 9.** Electorchromic behavior of **Ic** thin film (in $CH_3CN$ with 0.1 M TBAP as the supporting electrolyte) at 0.95 (★), 1.00 (○), 1.05 (△), 1.10 (▽), 1.15 (◇), 1.20 (◁), 1.25 (▷), 1.30 (□), and 1.35 (☆) (V versus $Ag/Ag^+$) for second stage oxidation. [Color figure can be viewed in the online issue, which is available at www.interscience.wiley.com.]

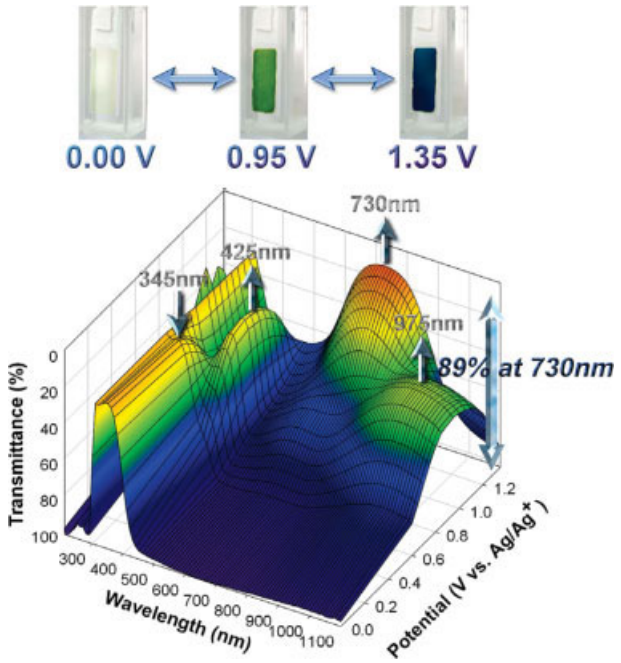


**Figure 10.** 3D spectroelectrochemical behavior of the **Ic** thin film on the ITO-coated glass substrate (in $CH_3CN$ with 0.1 M TBAP as the supporting electrolyte from 0.00 to 1.35 (V versus $Ag/Ag^+$).

determined from the *in situ* experiments.[30] The results presented herein also demonstrate that incorporation of bulky cardo fluorene group into polymer backbone results in polymer with light-color in the visible light region, thus enhanced coloration efficiency with higher contrast of the corresponding electrochromic materials.

The spectroelectrochemical spectra and the color switching time were conducted 1000 cyclic scans by applying a potential step between 0.0 and 0.85 V and exhibited excellent electrochromic reversibility (Fig. 11). The switching time was defined as the time that required for reach 90% of the full change in absorbance after switching potential. The thin films from polyamide **Ic** would require 3.7 s at 0.85 V for switching absorbance at 425 and 975 nm and 1.75 s for bleaching, and required 1.9 s for coloration at 730 nm and 1.0 s for bleaching when the potential was set 1.35 V. After over 1000 cyclic scans (Fig. 11), the polymer films still exhibited good stability of electrochromic characteristics. The electrochromic coloring efficiency ($\eta=\delta OD_{425}/Q$) ranging from 299 $cm^2/C$ for 1st cycle to 260 $cm^2/C$ for 1000th cycles with excellent stability of electrochromic behavior and decay of the polyamide **Ic** were calculated[31] and the results are summarized in Table 6.

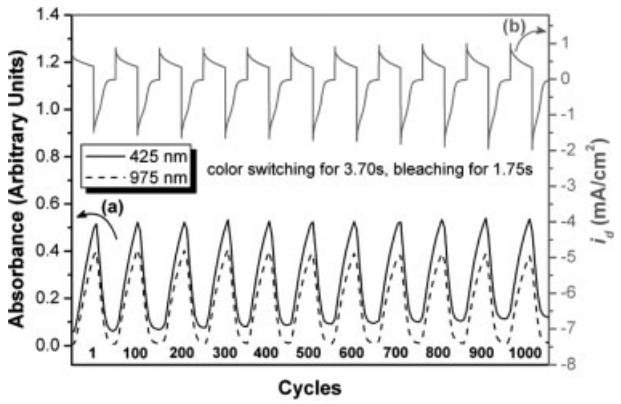


**Figure 11.** (a) Potential step absorptometry and (b) current consumption of the polyamide **Ic** film on to the ITO-coated glass substrate (coated area: 1 $cm^2$) during the continuous cycling test by switching potentials between 0.00 and 0.85 V (versus $Ag/Ag^+$).

**Table 6.** Coloration Efficiency with Optical and Electrochemical Properties of Polyamide **Ic**

| Cycles[a] | $\delta OD_{425}$[b] | $Q$ ($mC/cm^2$)[c] | $\eta$ ($cm^2/C$)[d] | Decay (%)[e] |
|---|---|---|---|---|
| 1 | 0.457 | 1.53 | 299 | 0 |
| 100 | 0.461 | 1.57 | 294 | 1.7 |
| 200 | 0.457 | 1.56 | 293 | 2.0 |
| 300 | 0.455 | 1.57 | 290 | 3.0 |
| 400 | 0.446 | 1.55 | 288 | 3.7 |
| 500 | 0.438 | 1.54 | 284 | 5.0 |
| 600 | 0.433 | 1.56 | 278 | 7.0 |
| 700 | 0.429 | 1.59 | 270 | 9.7 |
| 800 | 0.433 | 1.63 | 266 | 11.0 |
| 900 | 0.436 | 1.65 | 264 | 11.7 |
| 1000 | 0.432 | 1.66 | 260 | 13.0 |

[a] Times of cyclic scan by applying potential steps: 0.00 ↔ 0.85 (V vs. $Ag/Ag^+$).
[b] Optical density change at 425 nm.
[c] Ejected charge determined from the *in situ* experiments.
[d] Coloration efficiency is derived from the equation: $\eta = \delta OD_{425}/Q$.
[e] Decay of coloration efficiency after cyclic scans.

## CONCLUSIONS

Three series of organo-soluble fluorine-containing aromatic polyamides, polyesters, and poly(1,3,4-oxidiazole)s were prepared from 9,9-bis(4-caboxyphenyl)fluorene (**2**) and various aromatic compound via the direct polycondensation. The introduction of the cardo fluorene moiety into the polymer backbone not only could effectively enhance the solubility and thin-film-form-

ing ability but also improve thermal stability. These polymers also exhibited UV-Vis absorption bands at 266–348 nm in DMAc solution, and their photoluminescence spectra showed maximum bands at 368–457 nm in the purple to green region. The thin films of aromatic polymers showed high optical transparency from UV-Vis transmittance measurement with cutoff wavelength in the range of 296–391 nm. The poly(amine-amide) **Ic** exhibited excellent electrochromic contrast and coloration efficiency, changing color from the colorless neutral form to green and then to the dark blue oxidized forms when scanning potentials positively from 0.00 to 1.35 V with good stability of electrochromic characteristics.

The authors are grateful to the National Science Council of the Republic of China for financial support of this work.

## REFERENCES AND NOTES

1. Pei, Q.; Yang, Y. J Am Chem Soc 1998, 118, 7416.
2. Leclerc, M. J Polym Sci Part A: Polym Chem 2001, 39, 2867.
3. Grice, A. W.; Bradeley, D. D. C.; Bernius, M. T.; Inbasekaran, M.; Wu, W. W.; Woo, E. P. Appl Phys Lett 1998, 73, 629.
4. Shu, C. F.; Dodda, R.; Wu, F. I.; Liu, M. S.; Jen, A. K. Y. Macromolecules 2003, 36, 6698.
5. Scherf, U.; List, E. J. W. Adv Mater 2002, 14, 477.
6. Yang, H. H. Aromatic High-Strength Fibers; Wiley: New York, 1989.
7. Imai, Y. High Perform Polym 1995, 7, 337.
8. Imai, Y. React Funct Polym 1996, 30, 3.
9. Cassidy, P. E. Thermally Stable Polymers Synthesis and Properties; Marcel Dekker: New York, 1980; p 179.
10. Nanjan, M. J. In Encyclopedia of Polymer Science and Engineering, Vol. 12; Mark, J. F.; Bikales, N. M.; Overberger, C. G.; Menges, G.; Kroschwitz, J. I., Eds.; Wiley: New York, 1988.
11. Eastmond, G. C.; Paprotny, J. Polymer 1999, 40, 46.
12. Espeso, J. F.; Campa, J. G.; Lozano, A. E.; Abajo, D. J. J Polym Sci Part A: Polym Chem 2000, 38, 1014.
13. Ge, Z.; Yang, S.; Tao, Z.; Liu, J.; Fan, L. Polymer 2004, 45, 3627.
14. Liou, G. S.; Yang, Y. L.; Su, O. Y. L. J Polym Sci Part A: Polym Chem 2006, 44, 2587.
15. Liou, G. S.; Chen, H. W.; Yen, H. J. J Polym Sci Part A: Polym Chem 2006, 44, 4108.
16. Liou, G. S.; Yen, H. J. J Polym Sci Part A: Polym Chem 2006, 44, 6094.
17. Liou, G. S.; Fang, Y. K.; Yen, H. J. J Polym Res 2007, 14, 147.
18. Song, S. Y.; Jang, M. S.; Shim, M. K.; Hwang, D. H.; Zyung, T. Macromolecules 1999, 32, 148.
19. Hwang, S. W.; Chen, Y. Macromolecules 2002, 35, 5438.
20. Barberis, V. P.; MikroyAnnidis, J. A. J Polym Sci Part A: Polym Chem 2006, 44, 3556.
21. Chen, S. H.; Chen, Y. J Polym Sci Part A: Polym Chem 2006, 44, 4514.
22. Wu, C. W.; Sung, H. H.; Lin, H. C. J Polym Sci Part A: Polym Chem 2006, 44, 6765.
23. Liou, G. S.; Hsiao, S. H.; Fang, Y. K. J Polym Sci Part A: Polym Chem 2006, 44, 6466.
24. Liou, G. S.; Hsiao, S. H.; Chen, W. C.; Yen, H. J. Macromolecules 2006, 39, 6036.
25. Cheng, S. H.; Hsiao, S. H.; Su, T. H.; Liou, G. S. Macromolecules 2005, 38, 307.
26. Vinogradova, S. V.; Reinisch, G.; Tur, D. R.; Ulrich, H.; Suprun, A. P.; Vointseva, I. I. Izvestiya Akad Nauk SSSR Seriya Khim 1975, 1, 191.
27. Demas, J. N.; Crosby, G. A. J Phys Chem 1971, 75, 991.
28. Su, T. H.; Hsiao, S. H.; Liou, G. S. J Polym Sci Part A: Polym Chem 2085, 2005, 43.
29. Kress, L.; Neudeck, A.; Petr, A.; Dunsch, L. J Electroanal Chem 1996, 414, 31.
30. Argun, A. A.; Aubert, P. H.; Thompson, B. C.; Schwendeman, I.; Gaupp, C. L.; Hwang, J.; Pinto, N. J.; Tanner, D. B.; MacDiarmid, A. G.; Reynolds, J. R. Chem Mater 2004, 16, 4401.
31. Mortimer, R. J.; Reynolds, J. R. J Mater Chem 2005, 15, 2226.